# Environmental Effects on the Stress Corrosion Cracking Behavior of an Additively Manufactured Stainless Steel

Jonathan Pegues[2,3], Michael Roach[1], R. Scott Williamson[1], Nima Shamsaei[2,3,*]

[1]*Department of Biomedical Materials Science, University of Mississippi Medical Center, Jackson, MS 39216*

[2]*Department of Mechanical Engineering, Auburn University, Auburn, AL 36849*

[3]*National Center for Additive Manufacturing Excellence (NCAME), Auburn University, Auburn, AL 36849*

*Corresponding author: shamsaei@auburn.edu

## Abstract

Additive manufacturing (AM) is becoming a more viable manufacturing process in the biomedical, aerospace, nuclear, and defense sectors as a means to fabricate near net shaped parts on demand. Austenitic stainless steels are gaining attention for AM of products for these applications due to their ease of fabrication, excellent corrosion resistance, and superior toughness. The performance of these alloys fabricated by AM techniques such as laser beam powder bed fusion has not been yet fully established. This research compares the microstructural characteristics and tensile stress corrosion cracking (SCC) of 316L stainless steel at room temperature and physiological temperature in distilled $H_2O$, salt water, Ringers, and spiked pH Ringers conditions.

**Keywords:** Stress corrosion cracking, environmentally assisted cracking, austenitic stainless steel, tensile properties

## Introduction

Additive manufacturing is rapidly becoming a viable option for parts used across several sectors including biomedical and defense. In both of these applications, the part's resistance to environmentally assisted cracking (EAC) in chloride environments could be of critical concern. For biomedical applications, surgical implants can be subjected to corrosive attack particularly in the event of an infection where the bodies pH level can drop as low as five [1]. For defense applications, parts are often subjected to sea spray conditions across a broad range of temperatures depending on the location and time of year [2, 3].

It has been reported that stress corrosion cracking (SCC) could occur in any alloy system given non-optimal process conditions and environment [2]. Due to the layer-by-layer manufacturing and unique microstructure provided by AM techniques, the susceptibility of these

materials to SCC is unknown. While many studies have investigated the mechanical performance of biomedical/defense grade additive manufactured materials such as 316L stainless steel (SS) [4-7], systematic investigation into the stress corrosion cracking behavior are lacking in the literature.

In this study the susceptibility of laser powder bed fusion (LB-PBF) 316L SS to stress corrosion cracking (SCC) under slow strain rate (SSR) testing according to ASTM G129 [8] is investigated and compared to its wrought counterpart. Tests are performed in distilled H2O, Ringers solution, a pH spiked Ringers solution, and a 3.5% solution of NaCl. The ductility, strength, and time to failure are all investigated to assess the effect of each environment on the LB-PBF material for both room temperature (RT) and 37° C.

## Experimental Set-up

316L SS rods were fabricated horizontally on an EOS M290 using OEM recommended parameters. Before removal from the substrate, the parts were stress relieved at 400°C for 1 hr and furnace cooled to RT. Threaded grip test coupons were designed based on ASTM G129 and machined to the final dimensions shown in Figure 1.

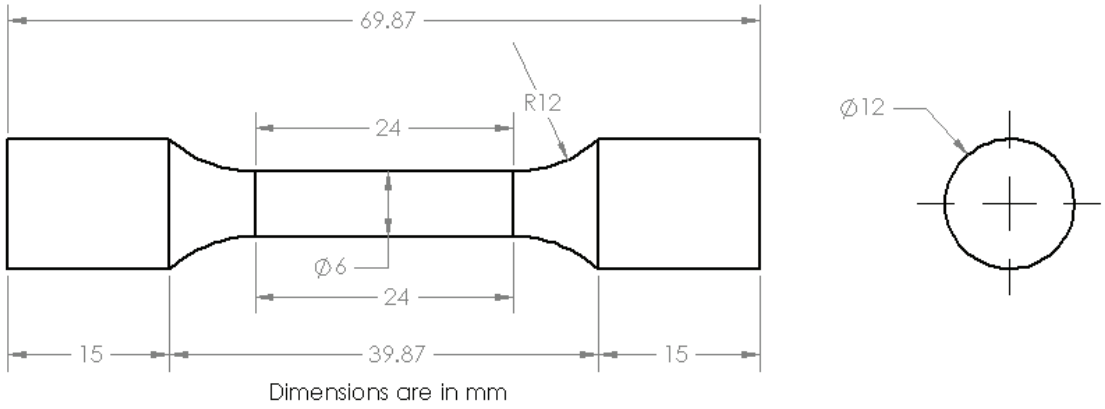


Figure 1: Specimen geometry used for slow strain rate testing.

Microstructural analysis was performed using both optical and scanning electron microscopy (SEM). Samples taken from the fabricated rods were polished using standard metallurgical procedures and electrolytically etched using a solution of nitric acid. Additional microstructure analysis was performed using electron backscatter diffraction (EBSD).

The SSR tensile tests were performed on an MTS servo-hydraulic load frame with a 100 kN capacity at a displacement stroke rate of $2.5*10^{-5}$ mm/s which resulted in an approximate strain rate of $1*10^{-6}$ $s^{-1}$. Tests were conducted either at RT or 37°C. Tests conducted in both Ringers and spiked pH Ringers were done only at 37°C while the distilled H2O and 3.5% NaCl were conducted at both RT and 37°C. Test specimens were completely submerged in the test solution and the temperature was monitored and controlled using a Digi-Sense temperature controller. Figure 2 gives a representation of the test setup used for this study. All samples were tested until failure,

after which, a measuring microscope was used to determine the elongation to failure and reduction of area (RoA).

Fracture surfaces were then examined with both a Keyence digital microscope and a Zeiss scanning electron microscope (SEM). Ratios between the control environment and the harsh environment were calculated by dividing the mean values of samples in harsh environments by the mean values of the samples in the control (distilled $H_2O$) at room temperature. ASTM G129 [8] states that ratios that are less than unity are considered to be susceptible to SCC. For this study a more strict definition of ratios falling below 0.9, which has been used in previous studies [9, 10], is considered to be susceptible to SCC.

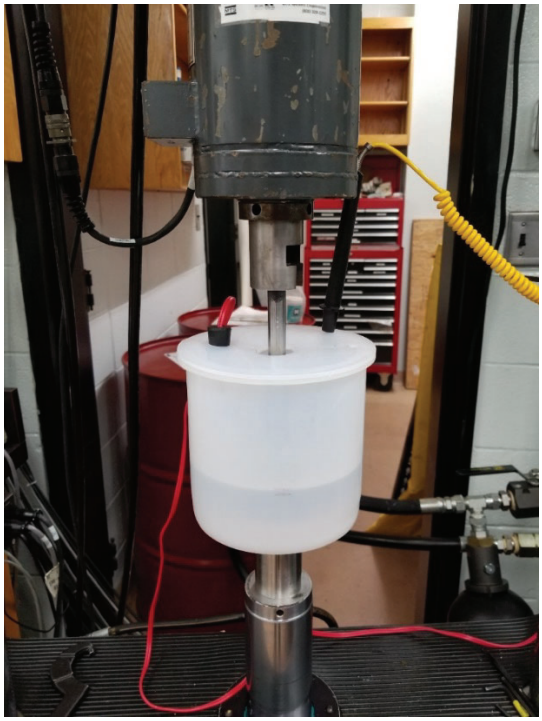

Figure 2: Test set up showing specimen submerged in solution during testing.

## Results

The microstructure of the LB-PBF 316L SS showed strikingly different morphology compared to the wrought counterpart, as shown in Figure 3. The microstructure of the wrought material is characterized by approximately 13 μ m equiaxed grains with a high density of annealing twins which can be recognized by the specific misorientation across the grain boundary. Σ 3 twin boundaries are low energy, mostly coherent grain boundaries which have a specific misorientation of 60° which can vary a few degrees by the Brandon criteria. The LB-PBF material, on the other hand, shows approximately 7 μ m non-equiaxed grains and a low density of annealing twins. In

contrast to the wrought material, the LB-PBF has a much higher density of low angle grain boundaries. Porosity was also observed for the LB-PBF material while unsurprisingly being absent from the wrought material.

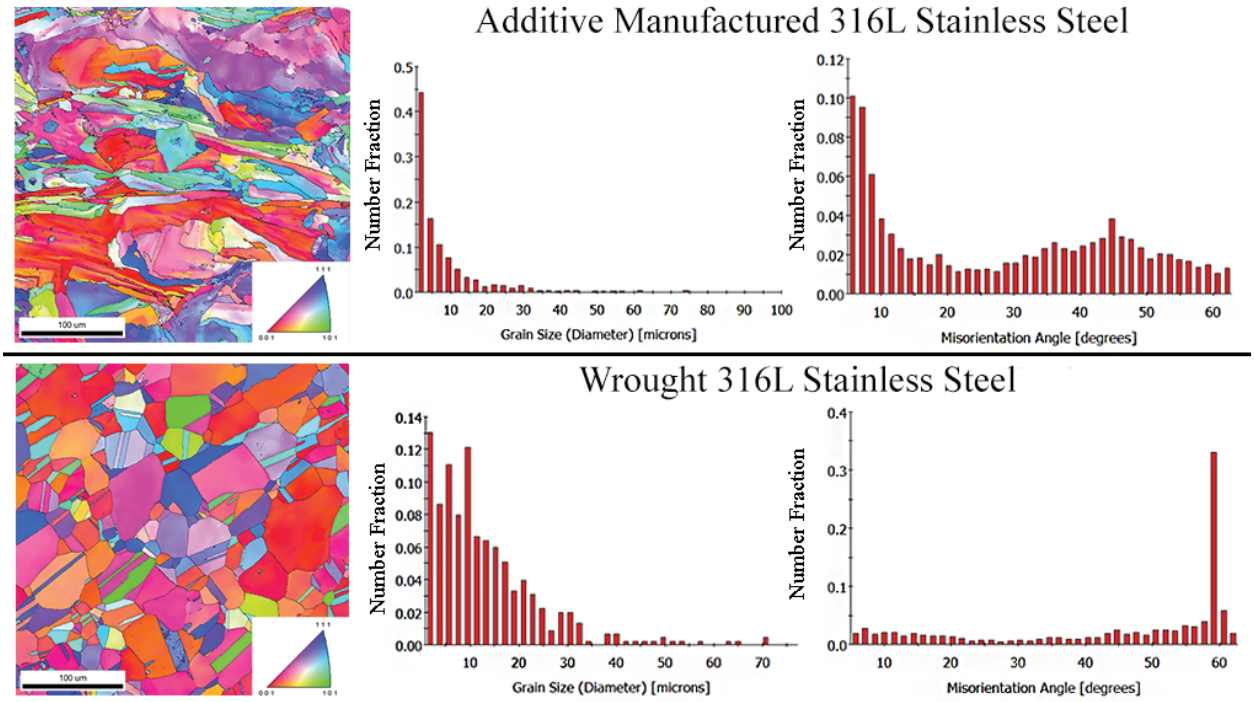


Figure 3: Microstructure of additive manufactured and wrought 316L stainless steel.

The stress-displacement curves for LB-PBF and wrought material in distilled H2O at both RT and 37°C is given in Figure 4. The LB-PBF condition showed higher yield stress ($\sigma_y$) and ultimate tensile stress (UTS) accompanied by lower elongation to failure. The improved strength of the LB-PBF material in most likely a result of the finer microstructure, i.e. grain boundary strengthening.

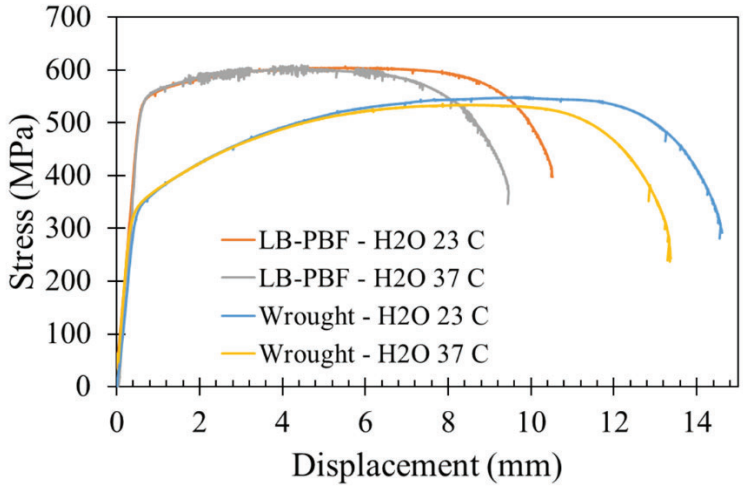


Figure 4: Stress-displacement curves for LB-PBF and wrought material at both room temperature and 37°C.

The fracture surfaces of the failed specimens gave no indication of brittle fracture for any of the test environments. Figure 5 gives a representation of select environments and temperatures. While all environments and temperature combinations are not covered in this image, the results show little to no indication of brittle failure. In both wrought and LB-PBF and all environmental conditions, the typical fibrous and ductile shear failure areas were observed. The LB-PBF material did show larger void growth which can be seen as the porous looking areas on the fracture surface. This is most likely due to the presence of the process induced porosity and could be leading to the lower elongation to failure observed for the LB-PBF material.

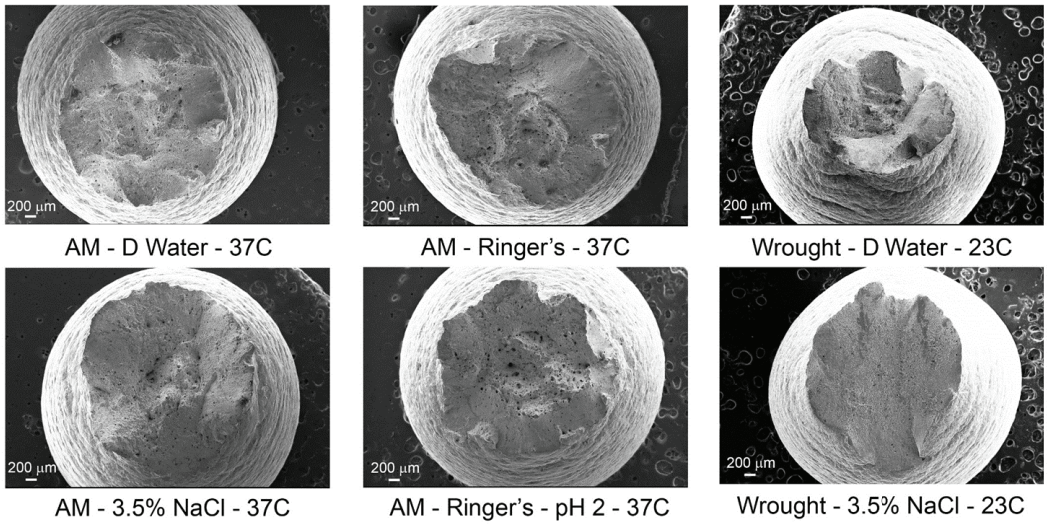


Figure 5: Fracture surfaces of select specimens in various environments and temperatures.

The SSR SCC tensile results for both AM and Wrought in all environmental conditions and temperatures are shown in Figure 6a-d. Similar to the stress-displacement curves shown in Figure 6a, the elongation to failure is lower for all AM tests regardless of environment with the 23°C tests showing slightly higher elongation to failure than the 37°C tests. Interestingly, while elongation to failure and reduction of area (ROA) are both measures of ductility, the ROA did not show the same temperature dependence that was observed for elongation to failure, as shown in Figure 6b. The difference between the AM and wrought material, however, was still evident. Time to failure (TTF) for each condition is shown in Figure 6c and, following the observations made for elongation to failure, the AM material showed much lower TTF than the wrought material with the 23°C showing slightly higher TTF than the 37°C tests. Lastly, the UTS for each condition is shown in Figure 6d. The AM material actually showed slightly higher UTS than the wrought material with no temperature dependence being evident for any condition.

(a)

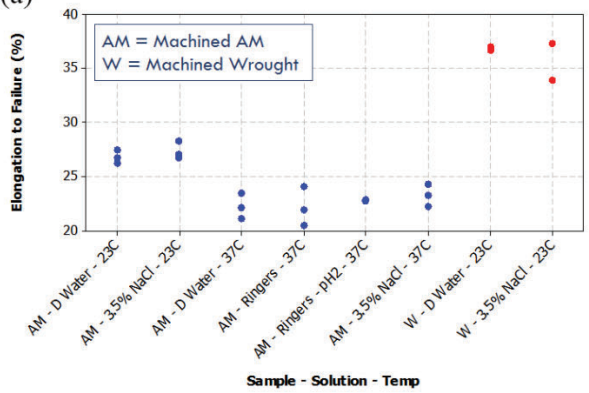
AM = Machined AM
W = Machined Wrought
Elongation to Failure (%)
40
35
30
25
20
AM - D Water - 23C
AM - 3.5% NaCl - 23C
AM - D Water - 37C
AM - Ringers - 37C
AM - Ringers - pH2 - 37C
AM - 3.5% NaCl - 37C
W - D Water - 23C
W - 3.5% NaCl - 23C
Sample - Solution - Temp

(b)

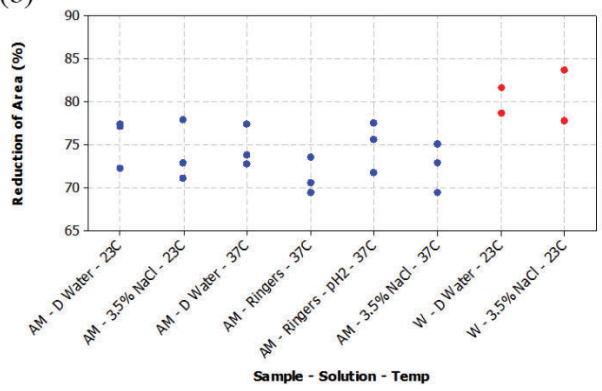
Reduction of Area (%)
90
85
80
75
70
65
AM - D Water - 23C
AM - 3.5% NaCl - 23C
AM - D Water - 37C
AM - Ringers - 37C
AM - Ringers - pH2 - 37C
AM - 3.5% NaCl - 37C
W - D Water - 23C
W - 3.5% NaCl - 23C
Sample - Solution - Temp

(c)

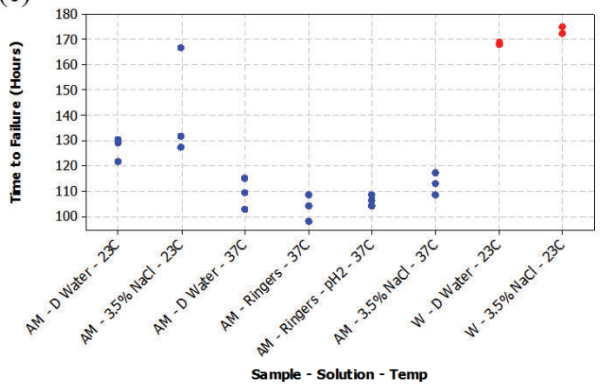
Time to Failure (Hours)
180
170
160
150
140
130
120
110
100
AM - D Water - 23C
AM - 3.5% NaCl - 23C
AM - D Water - 37C
AM - Ringers - 37C
AM - Ringers - pH2 - 37C
AM - 3.5% NaCl - 37C
W - D Water - 23C
W - 3.5% NaCl - 23C
Sample - Solution - Temp

(d)

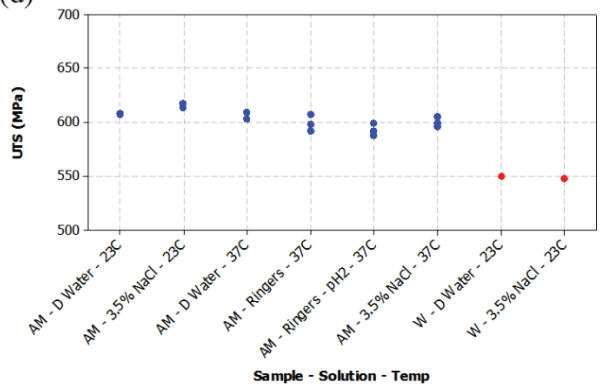
UTS (MPa)
700
650
600
550
500
AM - D Water - 23C
AM - 3.5% NaCl - 23C
AM - D Water - 37C
AM - Ringers - 37C
AM - Ringers - pH2 - 37C
AM - 3.5% NaCl - 37C
W - D Water - 23C
W - 3.5% NaCl - 23C
Sample - Solution - Temp

To assess the susceptibility of EAC under SSR testing, ASTM G129 requires the comparison SSR ratios of the chloride environment to the control. Decreasing SSR ratios can be indicative of susceptibility to stress corrosion cracking with ratios that drop below 0.9 showing a higher sensitivity to the harsh environment. Table 1 list all ratios for each condition compared to its control. It is important to note that the condition can only be compared to a control with similar conditions. For example, the AM test conducted at 23°C in 3.5% cannot be compared to the control (distilled H2O) for AM conducted at 37°C or with the control for wrought at 23°C. Surprisingly, Table 1 shows that the AM condition shows very little susceptibility to chloride environments as all ratios are greater than or equal to 0.95. This is similar to what was shown for the wrought condition at 23°C in 3.5% NaCl.

Table 1: Failure ratios for all test conditions.

| Sample Type | Test Temp. | Test Solution | Elongation to Failure Ratio (ELR) | Reduction of Area Ratio (ROAR) | Time to Failure Ratio (TTFR) |
|---|---|---|---|---|---|
| AM Machined | 23C | D Water | 1.00 | 1.00 | 1.00 |
| | 23C | 3.5% NaCl | 1.02 | 0.98 | 1.12 |
| | 37C | D Water | 1.00 | 1.00 | 1.00 |
| | 37C | Ringer's | 1.00 | 0.95 | 0.95 |
| | 37C | Ringer's – pH 2 | 1.03 | 1.00 | 0.98 |
| | 37C | 3.5% NaCl | 1.05 | 0.97 | 1.04 |
| Wrought Machined | 23C | D Water | 1.00 | 1.00 | 1.00 |
| | 23C | 3.5% NaCl | 0.97 | 1.01 | 1.03 |

## Conclusions

Results from this preliminary study indicate that the LB-PBF material does not show susceptibility to SCC under the tested conditions. While the tensile behavior of the LB-PBF material shows large differences compared to the wrought material, there was little to no evidence of brittle fracture on the fracture surfaces related to EAC. Additionally, ratios of the tensile properties compared to the control were essentially unity, indicating that SCC behavior was significantly different between the control and harsh environment. These results, while positive,

show the promising potential additive manufactured austenitic stainless steels in harsh environments. It must be noted, however, that while slow strain rate testing can be useful in determining the susceptibility of materials to SCC, the service life of these parts are often vastly longer than what takes place during this test method. Additionally, the fatigue properties of materials used in harsh environments is often more sensitive and, therefore, more rigorous studies are needed to fully understand the effect of EAC on these materials.

## Acknowledgements

Partial funding for this work was provided by the National Science Foundation under Grant No. 1657195. Supports from the Naval Air Systems Command (NAVAIR) is also greatly appreciated.

## References

[1] M. Sivakumar, S. Rajeswari, Investigation of failures in stainless steel orthopaedic implant devices: pit-induced stress corrosion cracking, Journal of Materials Science Letters 11(15) (1992) 1039-1042.

[2] B.F. Brown, Stress-corrosion cracking in high strength steels and in titanium and aluminum alloys, Naval Research Lab Washington DC, 1972.

[3] R.P. Wei, R.P. Gangloff, Environmentally assisted crack growth in structural alloys: perspectives and new directions, Fracture Mechanics: Perspectives and Directions (Twentieth Symposium), ASTM International, 1989.

[4] J.M. Jeon, J.M. Park, J.-H. Yu, J.G. Kim, Y. Seong, S.H. Park, H.S. Kim, Effects of microstructure and internal defects on mechanical anisotropy and asymmetry of selective laser-melted 316L austenitic stainless steel, Materials Science and Engineering: A 763 (2019) 138152.

[5] B.M. Morrow, T.J. Lienert, C.M. Knapp, J.O. Sutton, M.J. Brand, R.M. Pacheco, V. Livescu, J.S. Carpenter, G.T. Gray, Impact of defects in powder feedstock materials on microstructure of 304L and 316L stainless steel produced by additive manufacturing, Metallurgical and Materials Transactions A 49(8) (2018) 3637-3650.

[6] R. Shrestha, J. Simsiriwong, N. Shamsaei, S.M. Thompson, L. Bian, Effect of Build Orientation on the Fatigue Behavior of Stainless Steel 316L Manufactured via a Laser-Powder Bed Fusion Process, Solid Freeform Fabrication 2016: Proceedings of the 26th Annual International Solid Freeform Fabrication Symposium (2016) 12.

[7] Z. Sun, X. Tan, S.B. Tor, C.K. Chua, Simultaneously enhanced strength and ductility for 3D-printed stainless steel 316L by selective laser melting, NPG Asia Materials 10(4) (2018) 127.

[8] A. G129, Standard practice for slow strain rate testing to evaluate the susceptibility of metallic materials to environmentally assisted cracking, (2013).

[9] R. Williamson, M. Roach, L. Zardiackas, Comparison of Stress Corrosion Cracking of Ti-15Mo, Ti-6Al-7Nb, Ti-6Al-4V, and CP Ti, J. Test. Eval (2004).

[10] M. Roach, R.S. Williamson, J. Pegues, N. Shamsaei, A Comparison of Stress Corrosion Cracking Susceptibility in Additively-Manufactured and Wrought Materials for Aerospace and Biomedical Applications.